

# Characterization of microstructure in silt-dominated sediments

Simon Oberhollenzer

*Institute of Soil Mechanics, Foundation Engineering and Computational Geotechnics/Graz University of Technology, Graz, Austria, s.oberhollenzer@tugraz.at*

Anna Fankhauser, Roman Marte, Franz Tschuchnigg

*Institute of Soil Mechanics, Foundation Engineering and Computational Geotechnics/Graz University of Technology, Graz, Austria, a.gollowitsch@student.tugraz.at, roman.marte@tugraz.at, franz.tschuchnigg@tugraz.at*

Michael Premstaller

*Premstaller Geotechnik ZT GmbH, Oberalm, Austria*

**ABSTRACT:** Fine-grained lacustrine sediments often show a wide range of stiffness and strength properties. On various construction sites in the area of Salzburg (Austria), characterized by silt-dominated soils, it has been observed that such soils often show unexpected low settlements under static loading on shallow foundations. On the other hand, significant settlements occurred sometimes in the context of deep foundation or soil improvement work. A possible explanation for such a behaviour could be related to the microstructure of these soils. Due to the difficulty related to undisturbed sample recovery, in-situ investigations, such as cone penetration tests, are becoming increasingly popular for the characterization of fine-grained soils in general and microstructure in detail. The present article demonstrates a statistical interpretation of in-situ measurements (CPT, CPTu, SCPT, SCPTu, SDMT), executed within the basin of Salzburg. Furthermore, the presence of microstructural bonds is indicated by means of CPT-based soil behaviour type charts for the Salzburger Seeton. Finally, an alternative procedure, based on the shear wave velocity is presented to determine the stiffness of structured silty sediments more realistically.

**Keywords:** silt, microstructure, stiffness, soil classification, Salzburger Seeton

## 1. Introduction

Postglacial sedimented soils, which are often characterized by a small stiffness, define the soil layering of various valleys in the area of the Alps. One of the most famous examples is the city of Salzburg, located close to the border to Germany (see Fig. 1) within the basin of Salzburg. The latter basin was formed during several glacial periods. The melting of the glaciers lead to a large lake within the basin which was filled during thousands of years mainly by fine-grain dominated sediments. Therefore, such (geologically) young sediments are often characterized by a high ground water table and are generally in a normally consolidated or slightly under consolidated state. Consequently, those sediments lead to an increased risk for building settlements due to their moderate stiffness and strength properties. In general, those unfavorable mechanical properties go hand-in hand with high extra costs for foundation and construction works or lead to frequent damages caused by building settlements.

On various construction sites in the area of Salzburg (Austria) it was observed that such soils often present unexpected low settlements under static loading on shallow foundations. On the other hand, significant settlements occurred sometimes in the context of deep foundation or soil improvement works. A possible explanation for such a behaviour could be related to microstructural bonds, which act in between soil particles. According to Robertson [1] thixotropy, secondary compression, cementation, cold welding and aging can cause these bonds (denoted

as structured soils). Compared to unstructured soils with the same void ratio, microstructure leads to an increased strength and stiffness up to a point where those bonds fail. In general, microstructural bonds might be destroyed easily due to large strains, weathering or dynamic stresses.

Due to the difficulty related to undisturbed sample recovery of soft to very soft soils for laboratory testing, in-situ investigations (i.e. cone penetration tests CPT or flat dilatometer tests DMT) - which allow rapid and cost-effective measurements over depth - are becoming increasingly popular in geotechnical engineering [2].

The cone penetration test (CPT) is one of the most popular in-situ tests. A probe is pushed under a constant rate of 2 cm/s into the soil. Simultaneously, the tip resistance  $q_c$  and the sleeve friction  $f_s$  are measured over depth. Additionally, the pore water pressure can be determined by means of a piezocone (CPTu). Thereby, the pore water pressure is usually measured above the cone at the position  $u_2$ . Furthermore, the soil's shear wave velocity  $V_s$  can be identified by means of seismic CPTu tests (SCPTu) for different depths [3].

In the past, soil behaviour type charts have been developed to characterize the soil type as well as the soil layering by means of in-situ measurements (tip resistance  $q_c$ , sleeve friction  $f_s$ , pore water pressure  $u_2$ , shear wave velocity  $V_s$ ). It should be noted, that these measurements are strongly influenced by geological processes, environmental impacts as well as physical and chemical processes. Consequently, regional experience is needed for an accurate interpretation of the results. In the last ten years intensive in-situ investigations by means of cone

penetration tests (CPT, CPTu and SCPTu) have been performed by Premstaller Geotechnik ZT GmbH within the basin of Salzburg. This article presents a statistical interpretation of a large dataset of in-situ tests (CPT, CPTu, SCPT and SCPTu) executed in the area of Salzburg. Furthermore, local differences are discussed by means of detailed interpretations of in-situ measurements ( $q_c$ ,  $f_s$ ,  $R_f = f_s/q_c$ ,  $V_s$ ). Additionally, soil behaviour type charts are utilized to characterize the test data with regard to the grain-size distribution of the sediments. Furthermore, application limits of soil behaviour type charts for silty soils are presented. In the last section of this paper, the stiffness of silty soils is discussed by applying existing correlations and a new approach based on seismic cone penetration tests (SCPTu).

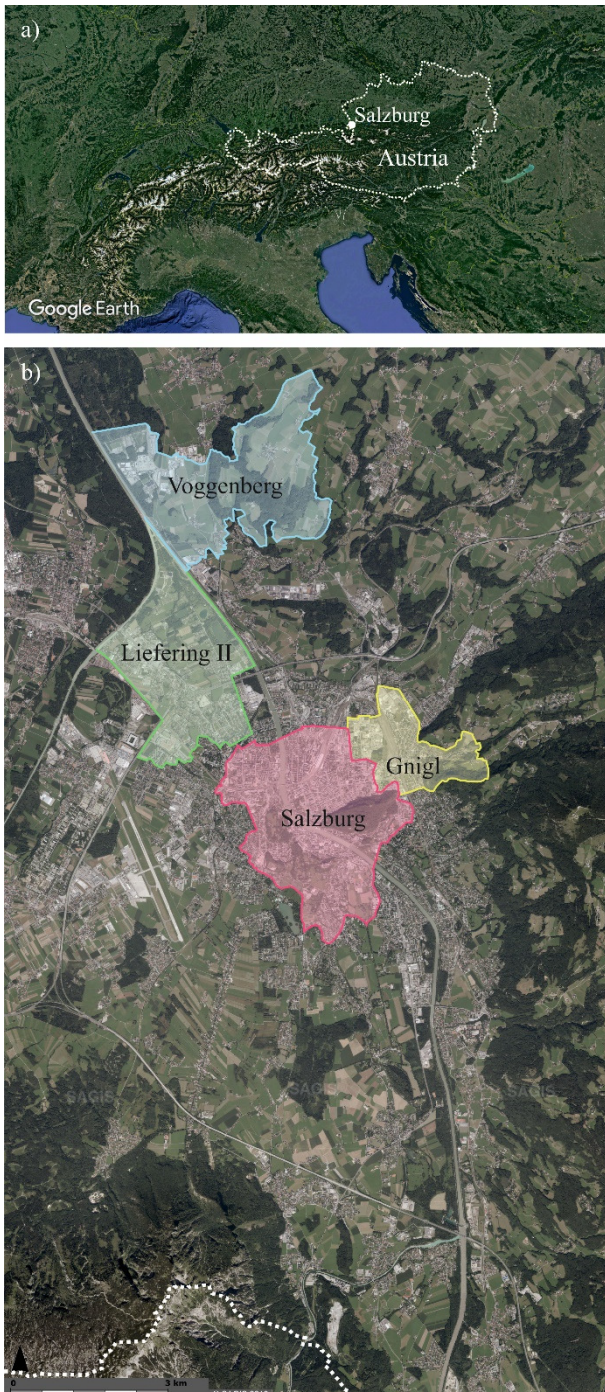


**Figure 1.** a.) Location of Salzburg - Austria; b.) Basin of Salzburg: Overview of the cadastral communities Salzburg, Gnigl, Liefering II, Voggberg

## 2. Database

In a first step 426 in-situ tests, executed by Premstaller Geotechnik ZT GmbH, were included into a QGIS data base [4]. As shown in Fig. 2, the in-situ tests were grouped in CPT (red symbol), CPTu (blue symbol) and seismic test (green symbol) layers. For each test several attributes (i.e. name, basin, location, country, cadastral community etc.) were defined. In-situ tests with a depth smaller than 3 meters are excluded from the current discussion. This decision is based on the fact that heterogeneous top layers and backfill materials generally dominate the first meters below subsurface. The data base can be subdivided into 250 CPT, 125 CPTu and 51 seismic tests (SCPT, SCPTu, SDMT). As shown in Fig. 3, most of the test results were executed within the cadastral communities "Salzburg", "Gnigl", "Voggberg" and "Liefering II". These areas represent the city center of Salzburg as well as very densely populated areas within the basin (see Fig. 1b). Therefore, local differences within the basin were elaborated using the mentioned cadastral communities (see Fig. 1b).



**Figure 2.** QGIS – extract of the data base: Overview of CPT (red), CPTu (blue), seismic tests (green), core drillings (violet)

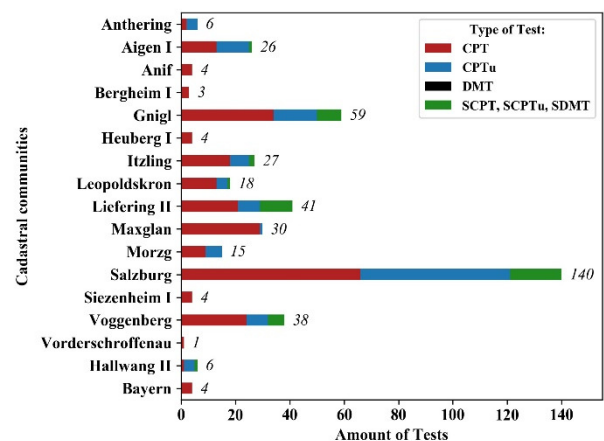


**Figure 3.** In-situ measurements for the different cadastral communities

Furthermore, 169 core drillings, located within a maximum distance of approximately 50 m from the in-situ tests, were included into the QGIS data base (violet symbols). Based on the soil description of the core drilling, the lithologic units of the neighbouring in-situ tests were defined using attribute tables.

### 3. In-situ measurements

#### 3.1. Basin of Salzburg

The typical geological stratigraphy within the basin of Salzburg can be divided into four main units: top layer, peat layer, floating sediments (fine sandy silt to silty fine sand) and a homogeneous clayey silt. It should be noted that the floating sediments and the clayey silt are the two unities of the so-called "Salzburger Seeton". The top layer, usually consisting of backfill material and gravel, is very heterogeneous and the tip resistance as well as the friction ratio differ strongly. As shown in Oberhollenzer et al. [2] the thickness of the top layer varies between a single meter and a couple of meters. Peat layers or lenses, with a thickness of approximately 1 to 3 m are often determined below the top layer. The peat is characterized by small tip resistances  $q_c < 1.5 \text{ MN/m}^2$  and large friction ratios  $R_f = 5$  to 6 %. The floating sediments, situated below the peat or top layer, consist of silty fine sands or fine sand-silt mixtures. Thin gravel lenses often separate the upper part of the Salzburger Seeton zonally. Consequently, the tip resistance  $q_c$  and friction ratio  $R_f$  vary within the layer. On the other hand, the lower part of the Salzburger Seeton is characterized by very homogeneous properties and can be addressed as clayey, fine sandy silt sometimes with thin interlayers of sand. Thereby, the tip resistance reduces strongly ( $q_c < 2 \text{ MN/m}^2$ ). The transition between the two unities of the Salzburger Seeton is located usually between 10 and 25 m below ground surface. Fig. 4 illustrates the discussed soil layers exemplarily for the project Röcklbrunnstraße (cadastral community of Salzburg).

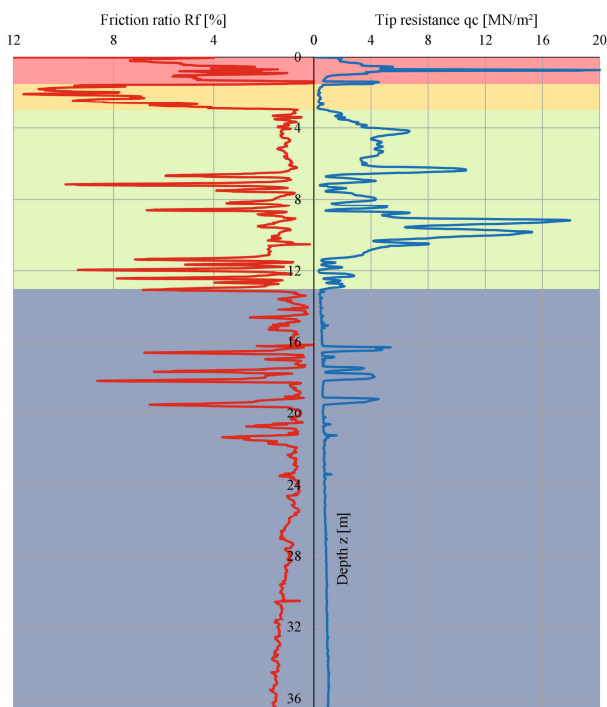


**Figure 4.** Soil layering within the basin of Salzburg (exemplary illustration from the project Röcklbrunnstraße): Top layer (red), Peat (yellow), Upper Seeton – floating sediments (green), lower Seeton – clayey, fine sandy silt (blue)

In a first step, the median, 25% and 75% quartiles as well as minimum and maximum values of the in-situ measurements were determined using the entire data base. Only a small number of in-situ tests were carried out deeper than 25 m below subsurface. In order to enable general statements, the discussion of results takes place to a depth equal to 25 m. The in-situ measurements ( $q_c$ ,  $f_s$ ,  $R_f$ ,  $V_s$ ) are presented in Fig. 5. It should be noted that the in-situ measurements are not normally distributed (Gaussian distribution) because the mean values and medians differ strongly. Therefore, the further discussions are performed by means of median, mean value, 25% quartile, 75% quartile, minimum and maximum value (box plot).

The medians (red lines) of the tip resistance  $q_c$  and sleeve friction  $f_s$  decrease with increasing depth (see Fig. 5). The tip resistance  $q_c$  in a depth equal to 5 m, 15 m and 20 m amount to 4.2 MPa, 1.7 MPa and 1.1 MPa respectively. In analogy, the sleeve friction  $f_s$  decreases from 45 kPa to 32.5 kPa and 11.1 kPa for the mentioned depths. Since the soil gets more homogeneous with increasing depth, the 25% quartile, 75% quartile as well as the difference between the minimum and maximum values of the tip resistance  $q_c$  decrease with increasing depth. This phenomenon is less pronounced for the sleeve friction  $f_s$ , because of a higher scatter in the measurements. Consequently, also the friction ratio  $R_f$  - which is calculated by means of tip resistance and sleeve friction - shows slightly decreasing quartile values with increasing depth (see Table 1). On the other hand, the  $R_f$  median values increase slightly with increasing depth, which indicates a higher fine-content in greater depths. Again, this is in good agreement with the decrease of  $q_c$  and  $f_s$  over depth. The shear wave velocity  $V_s$  presents a large scattering of the quartiles along the upper 10 m. In this section, the medians amount to approximately 190 to 250 m/s. With increasing depth, the quartiles decrease. Furthermore, the medians increase slightly due to the increase in stress level. Table 1 gives an overview of the in-situ measurements  $q_c$ ,  $f_s$ ,  $R_f$  and  $V_s$ .

#### 3.2. Local differences within the basin

Based on the holistic interpretation it was clarified that with increasing depth the sediments become more homogeneous and more fine-grained. On the other hand, the high values for the quartiles illustrate that the properties differ strongly within the basin. Therefore, the in-situ results ( $q_c$ ,  $R_f$  and  $V_s$ ) of four cadastral communities (Salzburg, Gnigl, Voggenberg and Liefering II) are compared to elaborate local differences within the basin of Salzburg. In the following, the medians and quartiles of the in-situ measurements are discussed. The in-situ measurements show similar tendencies for the different cadastral communities in Fig. 6. It is obvious that the medians as well as the quartiles of both tip resistance  $q_c$  and shear wave velocity  $V_s$  are higher within the first 7 to 15 meters. The  $q_c$  median values of Salzburg and Liefering II are in good agreement and are approximately 3.3 MPa and 3.7 MPa respectively. On the other hand, the median values within "Voggenberg" are higher, suggesting a coarser grain-size distribution or denser state ( $q_c$  median = 6.0 – 12.0 MPa).

Consequently, the shear wave velocity  $V_s$  is higher and the friction ratio  $R_f$  is lower within the first 8 to 10 m (compared to Salzburg and Liefering II). On the other hand it appears that the median and quartiles of  $q_c$  are significantly lower in Gnigl within the first 10 m ( $q_c$  median = 1.7 MPa). Therefore, shear wave velocities  $V_s$  are slightly lower and friction ratios  $R_f$  are higher compared to the other three cadastral communities. In the course of construction works, high settlements were frequently determined in Gnigl. This observation is in good agreement with the results of Fig. 6.

Based on the test results one can see that with increasing depth the median values of the tip resistance  $q_c$  decrease significantly for all cadastral communities. At a depth equal to 20 m below subsurface the medians of the cadastral communities amount to 1.0 MPa (Salzburg, Liefering II), 0.7 MPa (Gnigl) and 3.2 MPa (Voggenberg). Furthermore, it becomes obvious that

below 17 m the sediments within Salzburg and Gnigl become very homogeneous leading to small quartile values for the tip resistance  $q_c$ . The shear wave velocities  $V_s$  increase slightly within the homogeneous section between approximately 10 to 23 m below subsurface. The median values increase from 195 m/s (Salzburg), 209 m/s (Gnigl), 245 m/s (Voggenberg), 254 m/s (Liefering II) to 257 m/s (Salzburg), 264 m/s (Gnigl), 287 m/s (Voggenberg), 269 m/s (Liefering II) respectively. It can be seen that the measured shear wave velocities within Salzburg and Gnigl are slightly lower compared to the other two cadastral communities.

The comparison of four cadastral communities clearly shows that the properties as well as the sedimentation process differ within the basin of Salzburg, in particular within the upper 15 m of the same cadastral community.

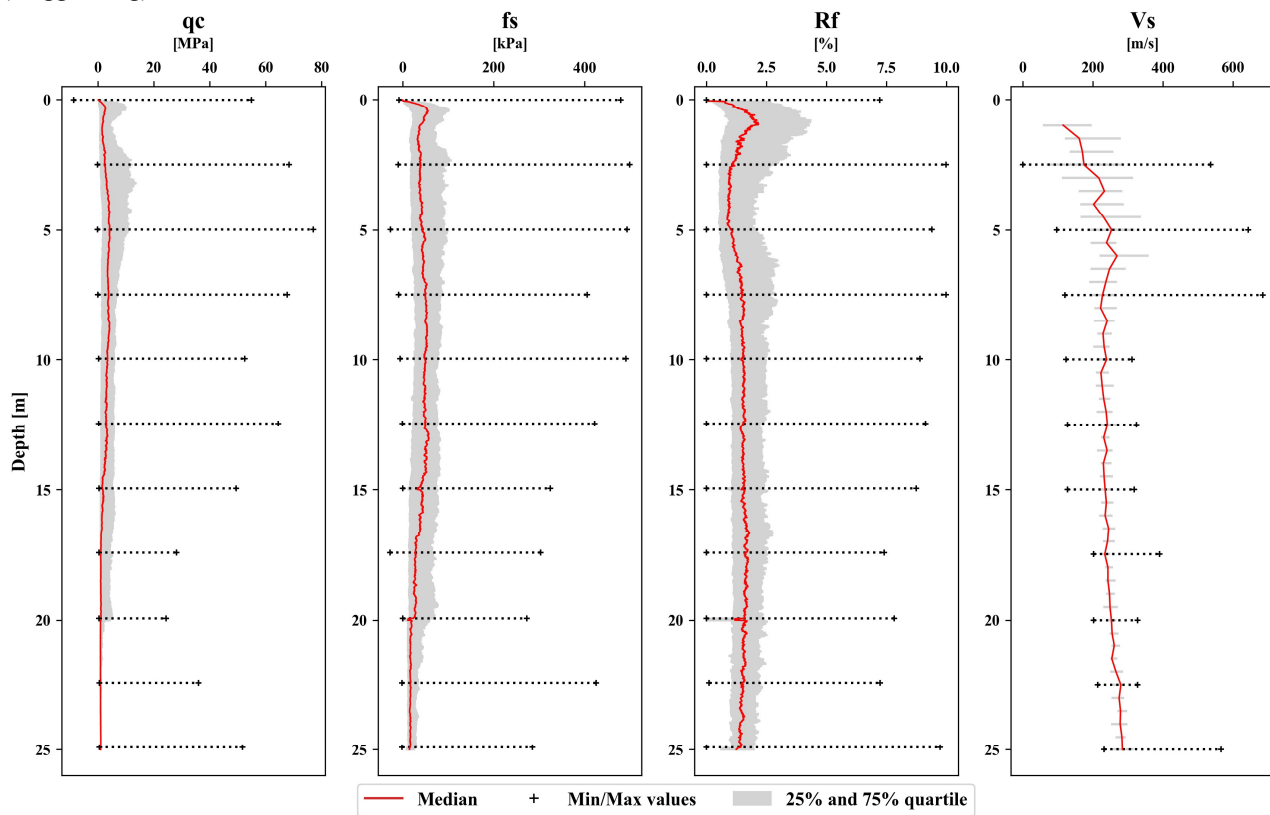


Figure 5. Comparison of the in-situ measurements within the basin of Salzburg

Table 1. Basin of Salzburg - Comparison of the in-situ measurements  $q_c$ ,  $f_s$ ,  $R_f$  and  $V_s$

Depth [m]	$q_c$ [MPa]			$f_s$ [kPa]			$R_f$ [%]			$V_s$ [m/s]		
	5	15	20	5	15	20	5	15	20	5	15	20
Median	4.2	1.7	1.1	45.0	32.5	11.1	1.0	1.4	1.6	253.5	235.0	253.0
25% quartile	1.5	0.8	0.7	20.8	11.0	0.0	0.6	0.9	1.0	187.8	217.5	244.8
75% quartile	10.5	5.6	4.7	89.8	75.1	35.1	2.0	2.2	2.3	318.8	251.8	267.0

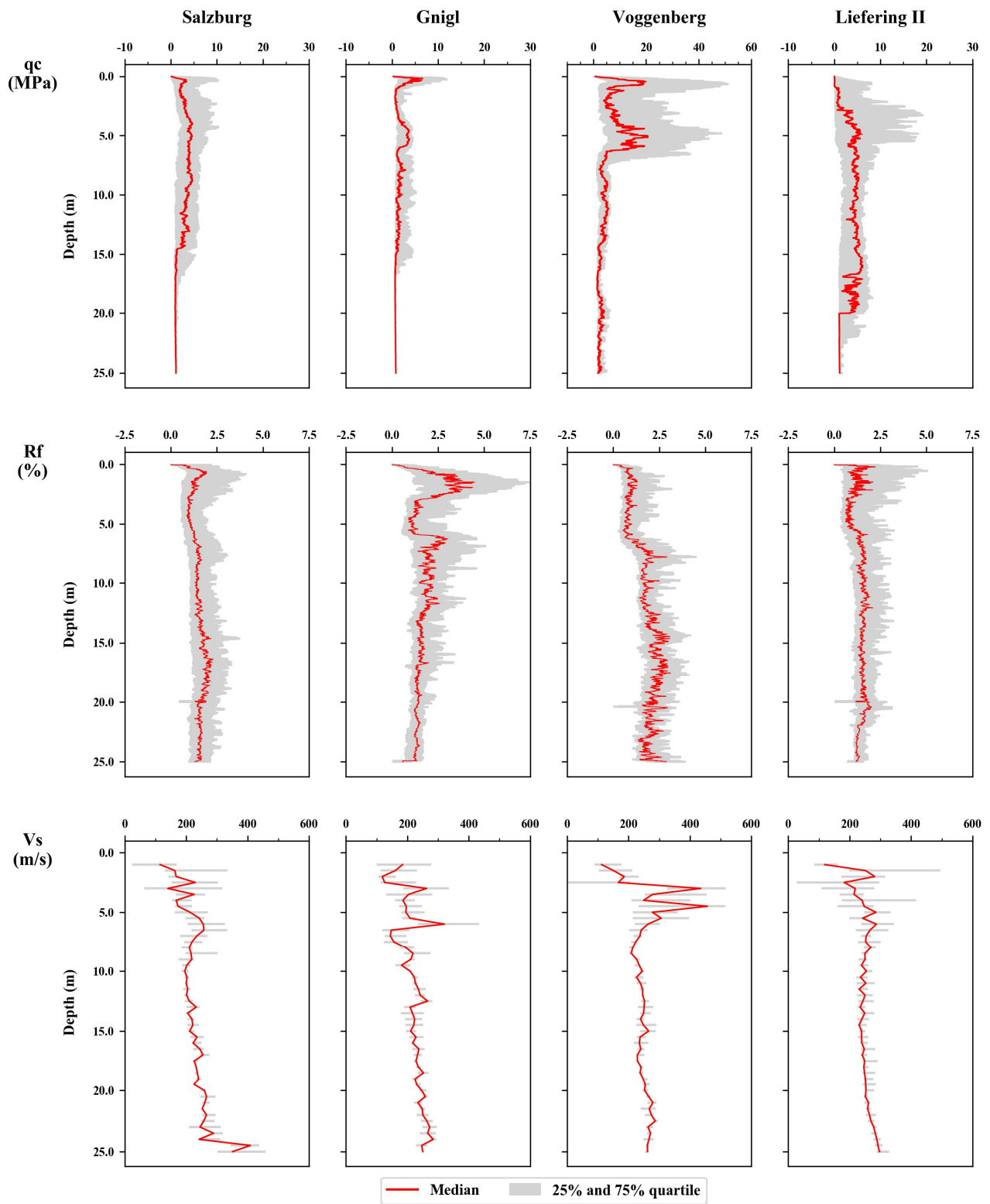


Figure 6. Comparison of the in-situ measurements for different cadastral communities within the basin of Salzburg

### 3.3. Characterization based on the grain-size distribution

The soil layering as well as the transition between the layers can differ within a basin and cadastral community. Consequently, there is a high risk that different grain-size distributions are compared to each other in a certain depth. Therefore, 426 in-situ tests (CPT, CPTu, seismic tests) executed within the basin of Salzburg were grouped according to their grain size and genesis (see Table 2). The classification was performed based on 169 core drillings executed within a maximum distance of 50 m to the in-situ tests. Based on this grouping the in-situ measurements are compared in the next step. The median values, mean values and quartiles of the tip resistance  $q_c$ , sleeve friction  $f_s$ , friction ratio  $R_f$  and shear wave velocity  $V_s$  are presented in Fig. 7 and Table 3.

**Table 2.** Classification of the soil according to the grain size distribution

Group	Grain-size distribution	Genesis
1	CSa → Gr	Top layer
2	Pt	Peat layer
3	FSa → CSa	Salzburger Seeton (upper)
4	Si, fsa → FSa, si	Salzburger Seeton (upper)
5	Si, cl- → Si, fsa-	Salzburger Seeton (lower)
6	Si, Cl → Si, cl	Salzburger Seeton (lower)

Soil group 1, mainly characterizing the top layer of the basin, covers the grain-size distributions between course sand and gravel (CSa → Gr). It's median values amount to  $q_c = 8.2$  MPa,  $f_s = 66.1$  kPa,  $R_f = 0.7\%$  and  $V_s = 255.0$  m/s. Furthermore, the means are clearly larger than the medians which confirms that no normal distribution is present. It becomes obvious that the 25% and 75% quartiles of all four in-situ measurements is higher compared to the other groups. This can be related to the

heterogeneity of the top layer. The peat layer (soil group 2) which is usually situated below the top layer is characterized by a low tip resistance  $q_c$ , sleeve friction  $f_s$ , shear wave velocity  $V_s$  and a high friction ratio  $R_f$ . The individual values are presented in Table 3.

Floating sediments - which represent the upper part of the Salzburger Seeton - mainly cover grain-size distributions between fine sandy silts (Si, fsa) and coarse sands (CSa). Therefore, the soil groups 3 and 4 can be assigned to this genesis. As shown in Figure 7, the mean values, medians and quartiles of the tip resistance  $q_c$ , sleeve friction  $f_s$  and friction ratio  $R_f$  of both groups are in good accordance. Furthermore, it can be seen that the  $q_c$ ,  $f_s$  and  $V_s$  are lower compared to the top layer but higher than the peat layer. This correlation can be interpreted inversely for the friction ratio  $R_f$ .

The soil groups 5 and 6 are part of the deeper situated Salzburger Seeton and cover grain-size distributions between silt-clay mixtures (Si,Cl) and fine sandy silts (Si,fsa). The 25 % and 75 % quartiles as well as the median values of group 6 are slightly smaller compared to group 5 due to the higher fines content. The tip resistance  $q_c$ , sleeve friction  $f_s$  and shear wave velocity  $V_s$  of groups 5 and 6 are clearly lower than for the upper part of the Salzburger Seeton. On the other hand, the friction ratio leads to a higher value because of the higher fines content. Furthermore, it becomes obvious that the lower Seeton is very homogeneous leading to small quartile values (see Table 3).

To sum up, it was shown that with increasing depth and fines content the tip resistance  $q_c$ , sleeve friction  $f_s$  and shear wave velocity  $V_s$  decrease and the friction ratio  $R_f$  increases. Hence, with increasing fines content the 25 % and 75% quartiles decreases. In this context, it is emphasized that the properties of the peat differs stronger. The mean values are significantly larger compared to the median values for all in-situ measurements.

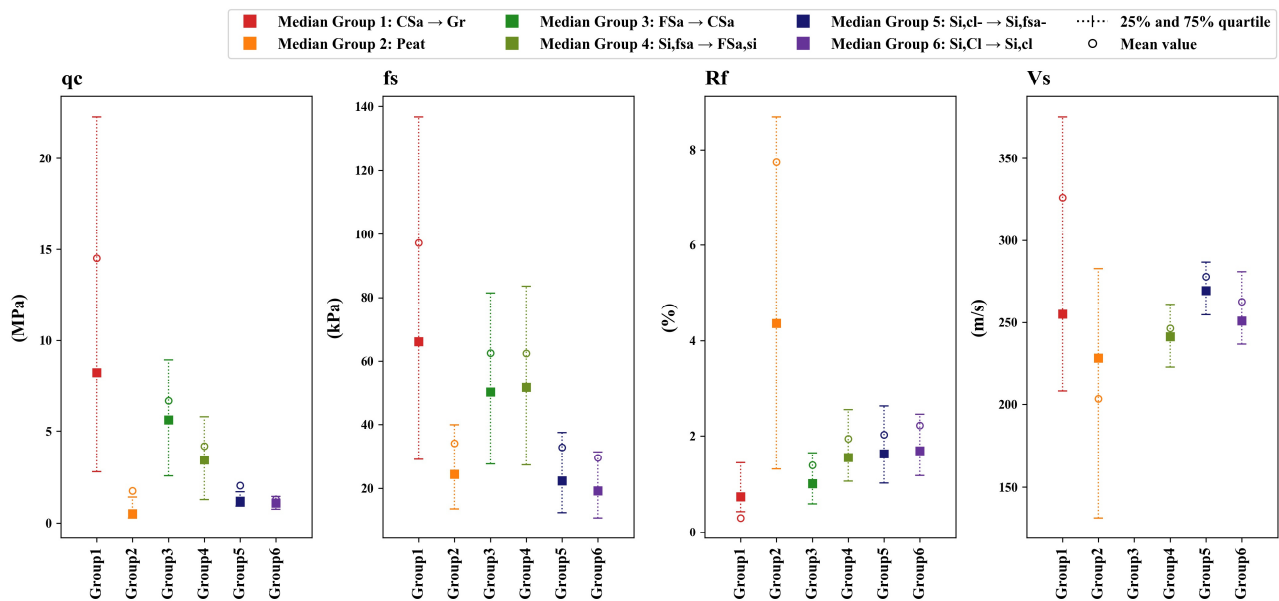


**Figure 7.** Comparison of in-situ measurements by means of the median, mean value, 25 % quartile and 75 % quartile for the groups listed in Table 2

**Table 3.** Overview of the median, mean value, 25 % quartile, 75 % quartile for the groups listed in Table 2

	$q_c$ [MPa]		$f_s$ [kPa]		$R_f$ [%]		$V_s$ [m/s]	
	Median	25% quartile	Median	25% quartile	Median	25% quartile	Median	25% quartile
	Mean value	75% quartile	Mean value	75% quartile	Mean value	75% quartile	Mean value	75% quartile
Group 1	8.2 / 14.5	2.8 / 22.3	66.1 / 97.2	29.0 / 136.8	0.7 / 0.3	0.4 / 1.4	255.0 / 326.0	208.0 / 375.0
Group 2	0.5 / 1.7	0.3 / 1.4	24.4 / 34.1	13.6 / 39.9	4.4 / 7.7	1.3 / 8.7	228.5 / 203.5	131.5 / 282.8
Group 3	5.6 / 6.7	2.6 / 8.9	50.1 / 62.6	27.6 / 81.5	1.0 / 1.4	0.6 / 1.7	-	-
Group 4	3.4 / 4.2	1.3 / 5.8	51.6 / 62.5	27.3 / 83.6	1.6 / 1.9	1.1 / 2.6	241.5 / 246.4	223.0 / 261.0
Group 5	1.2 / 2.0	0.9 / 1.7	22.3 / 32.8	12.5 / 37.4	1.6 / 2.0	1.0 / 2.6	269.5 / 277.9	254.8 / 286.8
Group 6	1.1 / 1.3	0.7 / 1.4	19.2 / 29.5	10.8 / 31.3	1.7 / 2.2	1.2 / 2.5	251.0 / 262.8	237.0 / 281.0

## 4. Soil classification by means of soil behaviour type charts

### 4.1. Soil behaviour type charts according to Robertson

In practical engineering the soil classification as well as soil layering are usually performed by means of CPT-based soil behaviour type charts. It should be noted that SBTn (normalized soil behaviour type charts) do not characterize the soil according to the grain-size distribution but according to their behaviour. Douglas and Olson [5] already showed that different soil types are represented by characteristic ratios between sleeve friction  $f_s$  and tip resistance  $q_c$ . Nowadays charts according to Robertson et al. [6] or Robertson [1][7] are widely used. The latter defines the soil using the normalized tip resistance  $Q_{tn}$  and the normalized friction ratio  $F_r$ :

$$Q_{tn} = [(q_t - \sigma_{v0})/p_a](p_a/\sigma'_{v0})^n \quad (1)$$

$$F_r = [f_s/(q_t - \sigma_{v0})]100\% \quad (2)$$

where  $q_t = q_c + u_2 \cdot (1-a)$  represents the tip resistance corrected for water effects;  $u_2$  is the pore water pressure measured above the cone;  $a$  is the cone area ratio determined by means of laboratory tests or calibration measures;  $p_a$  is the atmospheric reference pressure;  $\sigma_{v0}$  and  $\sigma'_{v0}$  represent the total and effective vertical in-situ stress respectively;  $n$  is a variable stress component. As shown in Fig. 8, Robertson [7] classifies the soil into the following nine groups: sensitive fine-grained, organic, clay, silt-mixtures, sand-mixtures, sand, gravelly sand to sand, very stiff sand to clayey sand, very stiff fine-grained. Furthermore, a sector for normally consolidated soils is defined by two blue dashed lines. This characterization is in good agreement with the European soil classification system (ISO 14688) for unstructured soils. For additional information reference should be made to Robertson [1].

Soils with a high normalized tip resistance ( $Q_{tn} > 12$ ) and a strong over consolidation ( $OCR > 4$ ) are often characterized by a dilative behaviour according to Robertson [7] and Mayne [8]. Therefore, Robertson [1] introduced a modified chart with a transition line between dilative and contractive behaviour ( $CD = 70$ ) within the  $Q_{tn}$ - $F_r$

space. All points which are situated below the  $CD = 70$  line are characterized by a contractive behaviour (see Fig. 9). Furthermore, hyperbolic boundaries - as recommended by Schneider et al. [9] - are used to distinguish between a clay-like, a transitional and a sand-like behaviour. As shown in Fig. 9, the lower boundary of the sand-like soils and the upper boundary of clay-like soils are defined by  $I_B = 32$  and  $I_B = 22$  respectively.  $I_B$ -values between 22 and 32 - determined based on  $Q_{tn}$  and  $F_r$  - define the transition zone between clay- and sand-like behaviours. Transitional soils are mostly characterized by partial drainage during the test execution [1]. The  $Q_{tn}$ - $F_r$  charts according to Robertson [1][7] were developed for unstructured soils which are characterized by no or rather weak microstructure.

Soils, formed by sedimentation processes (i.e. Salzburger Seeton), might be characterized by microstructural bonds, which act in between the soil particles and change the mechanical behaviour of the soil (see section 1). Those bonds lead to a rise of the small strain stiffness shear modulus  $G_0 (= \rho \cdot V_s^2)$  and the tip resistance  $q_c$ , whereby  $G_0$  increases stronger than  $q_c$  [3]. Therefore, Robertson [1] recommended seismic cone penetration tests (SCPT, SCPTu) to detect microstructural bonds. On this basis the  $Q_{tn}$ - $I_G$  chart shown in Fig. 10 was developed, where  $I_G$  presents the small-strain rigidity index. Based on the net resistance  $q_n = q_t - \sigma_{v0}$  and the small strain stiffness shear modulus  $G_0$  the small-strain rigidity index  $I_G$  can be calculated according to Eq. (3):

$$I_G = G_0/q_n \quad (3)$$

The empirical parameter  $K^*_G$  - based on  $G_0$ ,  $q_n$  and  $Q_{tn}$  - was defined by Robertson [1] to detect microstructure (see Fig. 10). Young soils with little or no microstructure are characterized by a  $K^*_G \sim 100$  and clearly  $< 330$ . On the other hand, soils which are characterized by microstructural bonds present a  $K^*_G$  factor  $> 330$ .

### 4.2. Classification of the Salzburger Seeton

In the following, in-situ measurements executed within the silt-dominated soils (groups 3, 4, 5 and 6) are discussed based on the normalized soil behaviour type charts according to Robertson [1][7].

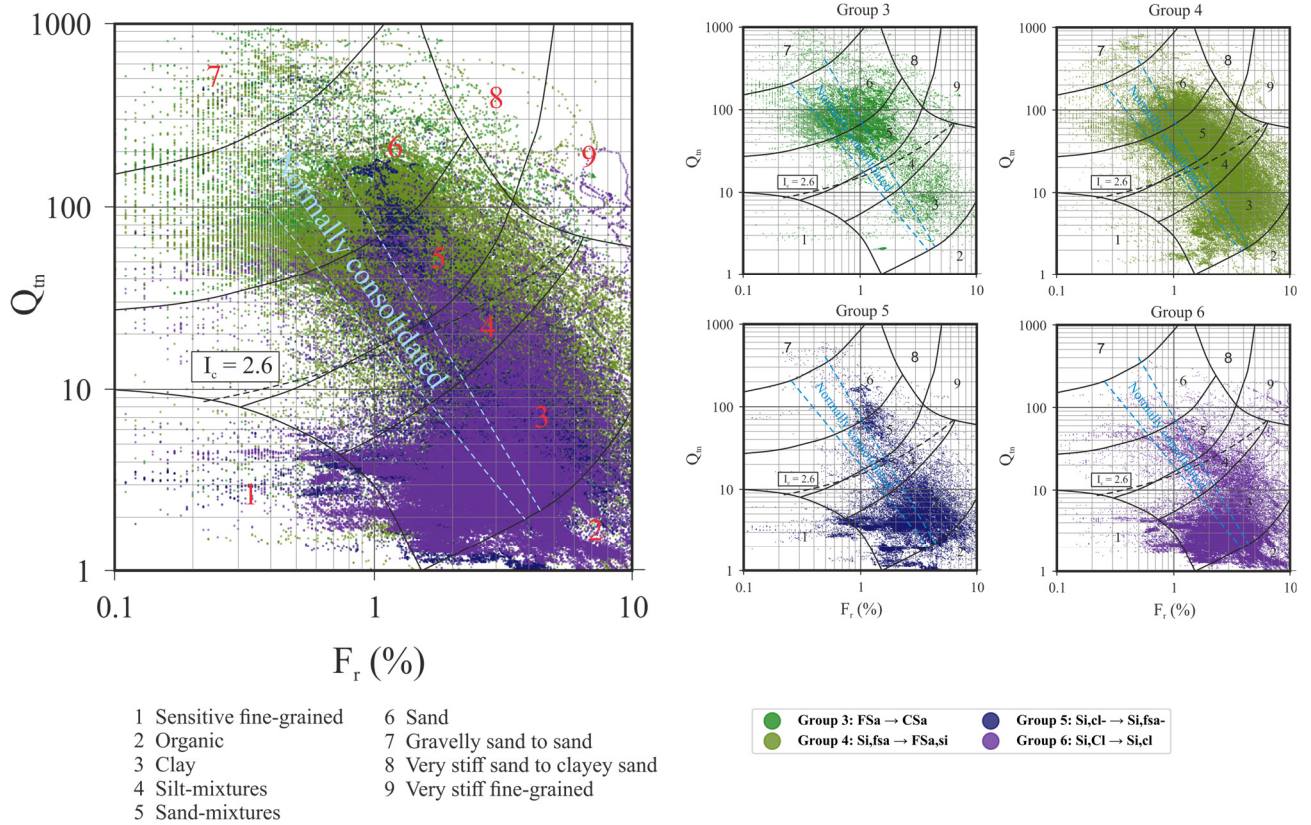


Figure 8. Soil behaviour type chart according to Robertson [7] – Comparison of results

One can see in Fig. 8 that the upper part of the Salzburger Seeton, primarily consisting of soil groups 3 (FSa → CSa) and 4 (Si,fsa → FSa,si), is mainly situated in the sections 3 to 6 (clay, silt-mixtures, sand-mixtures, sand) according to Robertson [7]. It is obvious that soil group 3 - which is defined by a coarser grain-size distribution compared to soil group 4 - is located primarily within the sections 5 (sand-mixtures) and 6 (sand). Soil group 3 is characterized by a sand-like dilative behaviour according to Robertson [1] (see Fig. 9). On the other hand, soil group 4 (Si,fsa → FSa,si) presents a larger scatter within the mentioned soil behaviour type chart varying between soil types 3 to 6 (see Fig. 8). Furthermore, this scatter of the in-situ measurement data for soil group 4 does not allow an assessment regarding its contractive or dilative behaviour in Fig. 9. Thin sand layers within the soil group 4 were often not defined as individual lithologies in the core drillings. This fact might be an explanation for a larger scatter of the test results.

The measurements of the deeper (=lower) part of the Salzburger Seeton (soil groups 5 and 6) are characterized by a homogeneous pattern and are mainly located within section 3 (clay) according to Robertson [7]. It should be noted that both soil groups 5 and 6 present very similar results (see Fig. 8, Fig. 9). Their behaviour is clay-like and contractive (CC) as shown in the updated soil behaviour type chart of Robertson [1] (see Fig. 9).

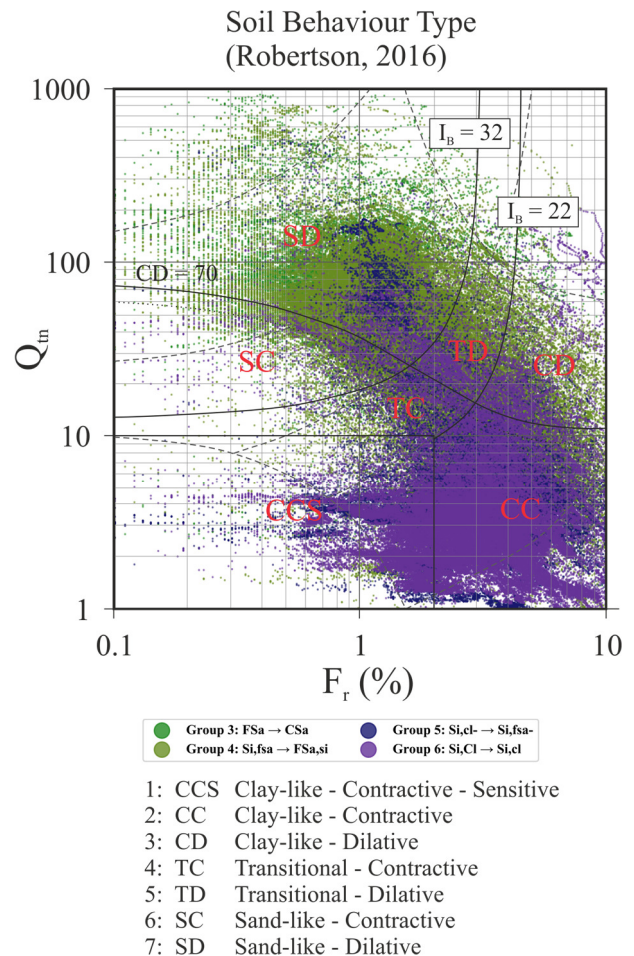
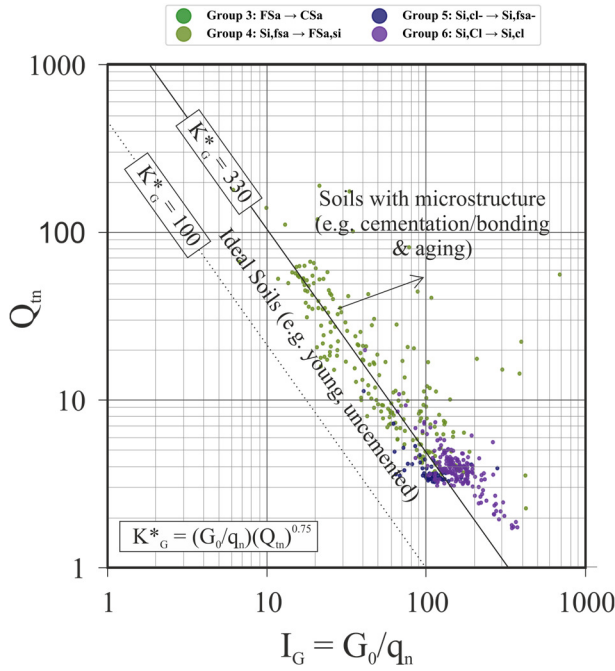


Figure 9. Soil behaviour type chart according to Robertson [1] – Comparison of the results



**Figure 10.** Soil behaviour type chart according to Robertson [1] – Detection of microstructure

In the following, the Salzburger Seeton (soil groups 3, 4, 5 and 6) is discussed by means of the  $Q_m$ - $I_G$  chart regarding the detection of microstructure. According to Robertson [1], the in-situ measurements presented within the  $Q_m$ - $I_G$  space (see Fig. 10) imply the presence of a microstructure for all four soil groups. Furthermore, the heterogeneous properties of the upper Salzburger Seeton (soil group 3 and 4) lead to a significant scatter of the in-situ measurements which are situated along the  $K^*_G \sim 330$  line. It should be noted that no shear wave velocity measurements were available for soil group 3. The results of the deeper situated Seeton (soil groups 5, 6) are characterized by a small measurement-noise and are mainly situated above the defined boundary  $K^*_G = 330$ . This indicates the presence of microstructural bonds according to Robertson [1].

The following relationships can be derived from the in-situ tests - executed within the basin of Salzburg - by means of soil behaviour type charts:

- The soil classification by means of soil behaviour type charts and core drillings are in good accordance for sand-dominated sediments. The soil behaviour type charts after Robertson [1][7] should be interpreted with caution as those only partially provide satisfactory results for silt dominated sediments.
- The Salzburger Seeton is mainly situated within and below the normally consolidated sector according to Robertson [7].
- In analogy to the in-situ measurements (see section 3) the soil behaviour type charts showed that with increasing depth, the subsoil gets more homogeneous. The soil groups 5 and 6 are characterized by a smaller scatter compared to the groups 3 and 4.
- The  $Q_m$ - $I_G$  chart indicates the presence of a microstructure in the deeper situated, homogeneous Salzburger Seeton (soil groups 5 and 6).

## 5. Stiffness of the Salzburger Seeton

### 5.1. Existing correlations for silty soils

Besides soil classification and soil layering, also the stiffness moduli are required for settlement predictions in practical engineering. In the past, various correlations have been developed to derive the oedometer stiffness based on the tip resistance  $q_c$ . Three approaches, applicable to silty soils, are discussed in the following:

Eq. (4) enables the determination of the constrained modulus (= oedometer stiffness) based on the tip resistance  $q_c$  and an  $\alpha$ -value. Recommended  $\alpha$ -values from literature are listed in Table 4. An enhanced correlation considering the overburden pressure is given in Eq. (5), where  $\sigma_{v0}$  is the total vertical stress.

$$E_S = \alpha \cdot q_c \quad (4)$$

$$E_S = \alpha \cdot (q_c - \sigma_{v0}) \quad (5)$$

A third stress dependent approach which has led to good accordance between in-situ and laboratory results is given by Eq. (6) [10]:

$$E_S = \nu \cdot p_a \cdot \left[ \frac{\sigma'_{v0} + 0.5 \cdot \Delta\sigma'_z}{p_a} \right]^w \quad (6)$$

where  $\sigma'_{v0}$  represents the effective vertical stress;  $\nu$  is the stiffness factor;  $w$  is the stiffness exponent ( $w = 0.6$  for fine-grained and  $w = 0.5$  for coarse grained soil);  $p_a$  is the atmospheric reference pressure and  $\Delta\sigma'_z$  represents the increase of the effective vertical stress due to the construction.

The stiffness factor  $\nu$  is equal to  $15.2 \cdot \log(q_c) + 50$  for fine grained soils ( $0.6 \leq q_c \leq 3.5$ ). For coarse-grained soils ( $5 \leq q_c \leq 30$ ) the factor depends on the coefficient of uniformity  $U$  (see Eq.(6) and Eq. (8)):

$$\text{For } U \leq 3 \rightarrow \nu = 167 \cdot \log(q_c) + 113 \quad (7)$$

$$\text{For } U > 6 \rightarrow \nu = 463 \cdot \log(q_c) - 13 \quad (8)$$

**Table 4.** Recommended  $\alpha$ -values from literature

Soil group	DIN 4094-1 [10]	Kulhawy and Mayne [11]
3 (FSa → CSa)	3.5 (fine and middle sand)	8.25
4 (Si,fsa → FSa,si)	2 (silty sand)	
5 (Si,cl → Si,fsa)	1-2 (plastic silt)	
6 (Si, Cl → Si, cl)	1-2 (plastic silt)	

### 5.2. Application

In the following, the correlations presented in section 5.1 (see Eq. (4), (5) and (6)) are evaluated for the upper and lower parts of the Salzburger Seeton. As shown previously, the subsurface conditions can differ strongly within the basin of Salzburg. Based on the measurements either soil groups 3, 4, 5 or 6 can be present in shallow depths. In the following, the stiffness moduli calculated

using Eq. (4), (5) and (6) are discussed based on the median values of  $q_c$  (see Table 3) in combination with the  $\alpha$ -values presented in Table 4. It should be noted, that for soil groups 5 and 6 the stiffness factor  $\nu$  for fine-grained soils was used (see Eq. (6)). On the other hand, for the soil groups 3 and 4 a coefficient of uniformity  $U \leq 3$  was used to determine the stiffness factor  $\nu$ . An overview of the resulting stiffnesses is given in Table 5. The black numbers correspond to  $\alpha$ -values according to DIN [10], the grey values are related to Kulhawy and Mayne [11] (see Table 5). As mentioned earlier, the listed values of Eq. (5) and (6) correspond to a vertical effective stress  $\sigma'_{v0} = 100$  kPa.

**Table 5.** Overview of calculated oedometer stiffnesses [MPa]

Correlation	Soil group 3	Soil group 4	Soil group 5	Soil group 6
Eq. (4)	19.6	6.8	1.2	1.1
	46.2	28.1	9.9	9.1
Eq. (5)	18.9	6.4	1.0	0.9
	44.6	26.5	8.3	7.5
Eq. (6)	24.0	20.4	5.2	5.1

The calculated constrained moduli based on Eq. (4) and (5) are in good agreement. This can be related to the low stress level and the assumed constant  $q_c$  values over depth. Eq. (6) leads to higher values compared to Eq. (4) and (5), when using  $\alpha$ -values according to DIN [10] in Eq. (4) and Eq. (5). The recommended  $\alpha$ -value according to Kulhawy and Mayne [11] increases the constrained modulus of soil group 3 about 135%. The increase is even more significant for the soil groups 4, 5 and 6 (300 – 700%). It should be noted that the  $\alpha$  - values, recommended in the literature differ strongly (see Table 4). Consequently, the determination of the constrained modulus  $E_s$  becomes very difficult.

### 5.3. Determination of stiffness by means of seismic cone penetration tests (SCPTu)

Since microstructural bonds of sediments (like the Salzburger Seeton) are very sensitive, they might be destroyed during the penetration procedure. Consequently, correlations based on the tip resistance  $q_c$  might not lead to realistic stiffness parameters considering an undisturbed microstructure. On the other hand, the propagation of the shear waves is non-destructive. Therefore, an alternative procedure to determine the stiffness of silty sediments by means of SCPT or SCPTu is discussed next.

As mentioned by Robertson [1], microstructural bonds lead to an expanded yield surface. Therefore, an unloading / reloading stiffness modulus should be considered for settlement analyses rather than a primary loading stiffness. On the other hand, reduced stiffness moduli are recommended if microstructural bonds are weakened or even destroyed. Based on the measured shear wave velocity  $V_s$  (using SCPTu, SDMT) the small strain stiffness shear modulus  $G_0$  can be derived according to Eq. (9):

$$G_0 = \rho \cdot V_s^2 \quad (9)$$

where  $\rho$  is the bulk density of the soil material.

Subsequently, an unloading/reloading reference stiffness  $E_{ur}^{ref}$  (e.g. Hardening Soil Small model [12]) can be calculated according to Eq. (10):

$$E_{ur}^{ref} = \frac{2 \cdot (1 + \nu_{ur}) G_0}{A} \quad (10)$$

where  $\nu_{ur}$  is the unloading / reloading Poisson's ratio and  $A$  is an empirical factor, which can vary between 2.5 and 10 [12].

In the following, a conservative factor  $A = 3$  is assumed. The calculated  $G_0$  and  $E_{ur}^{ref}$  values are listed in Table 6. It should be noted that the small shear wave velocity of soil group 4 can be related to a lower stress level compared to the soil groups 5 and 6.

**Table 6.** Stiffness parameters according to the alternative approach

	Soil group 4	Soil group 5	Soil group 6
$V_s$ median [m/s]	241.5	269.5	251.0
$G_0$ [MPa]	118.9	155.5	134.9
$E_{ur}^{ref}$ [MPa]	95.1	124.4	107.9
( $p_{ref} = 0.1$ MPa)			

## 6. Conclusions

A large data set of in-situ tests (CPT, CPTu, SDMT, SCPT, SCPTu) and core drillings executed within the basin of Salzburg was discussed in the current article. The most important findings can be summarised as follows:

- Soil properties within basins such as the basin of Salzburg can vary significantly. With increasing depth, the sediments are characterized by more homogeneous properties, so that the dispersion of the measured values (see decreasing quartile values) decreases. The median values of the tip resistance  $q_c$  and sleeve friction  $f_s$  decrease due to an increase of fines-content with depth.
- Based on the distribution of the tip resistance, friction ratio and shear wave velocity it can be concluded that the sediments within the cadastral communities "Salzburg" and "Gnigl" are characterized by a slightly smaller stiffness compared to "Voggenberg" and "Liefering II".
- The direct comparison of core drillings with penetration tests clarified that the soil behaviour type charts after Robertson [1][7] should be interpreted with caution as those only partially provide satisfactory results for silt dominated sediments.
- For settlement calculations in silty soils, correlations to determine stiffness parameters based on the tip resistance  $q_c$  differ strongly. Generally they show too low values compared to measured results from constructed buildings. In this context, a non-destructive approach based on the measured shear wave velocity leads to more realistic settlement predictions as long as the microstructural bonds are present. Although a deeper understanding of these bonds acting in between the soil particles is required.
- Microstructure might have a significant influence on the stress-strain behaviour of fine-grained sediments (i.e. Salzburger Seeton). This could explain

quite low settlements for static loadings and sometimes high settlements in context of dynamic loads due to vibrations during underground construction works.

Since Austrians post glacial formed basins are characterized by the appearance of silt dominated soils, a main goal is to improve the characterization of those sensitive soils. Therefore, the Chamber of Architects and chartered Engineering Consultants in cooperation with the Institutes of Soil Mechanics, Foundation Engineering and Computational Geotechnics and Applied Geosciences (Graz University of Technology) started the research project PITS “Parameter identification by means of in-situ tests in silty soils”.

## Acknowledgement

The project presented in this article is supported by the Austrian Research Promotion Agency (FFG) and the Federal Chamber of Architects and chartered Engineering Consultants (Austria).

## References

- [1] Robertson, P. K. „Cone penetration test (CPT)-based soil behaviour type (SBT) classification system — an update“, *Canadian Geotechnical Journal*, 53(12), pp. 1910-1927, 2016. <http://doi.org/10.1139/cgj-2016-0044>
- [2] Oberhollenzer, S., Marte, R., Gasser, D., Premstaller, M., Leitich, A. „Microstructure of the Salzburger Seeton – Characterization based on cone penetration tests“, *Geomechanics and Tunneling*, 12(4), pp. 340-351, 2019. <http://doi.org/10.1002/geot.201900012>
- [3] Schnaid, F. „In-situ testing in geomechanics – the main tests“, 1st ed., Taylor & Francis Group, London, England, 2009, pp. 120-124.
- [4] Athan, T., Ersts, P., Macho, W., Dassau, O. “QGIS User Guide (Release 2.18) – QGIS Project” [pdf] Available at: <https://docs.qgis.org/2.18/pdf/en/QGIS-2.18-UserGuide-en.pdf> [Accessed: 01.11.2019]
- [5] Douglas, B. J., Olsen, R. S. “Soil classification using electric cone penetrometer”, In: *Symposium on Cone Penetration Testing and Experience*, St. Louis, Missouri, 1981, pp. 209-227.
- [6] Robertson, P. K., Campanella, R. G., Gillespie, D., Greig, J. “Use of piezometer cone data”, In: *In-Situ’86 - Use of In-situ Tests in Geotechnical Engineering*, Blackburg, Virginia, 1986, pp. 1263-1280.
- [7] Robertson, P. K. “Interpretation of cone penetration tests – a unified approach”, *Canadian Geotechnical Journal*, 46(11), pp. 1337–1355, 2009. <http://doi.org/10.1139/T09-065>.
- [8] Mayne, P. W. “Interpretation of geotechnical parameters from seismic piezocone tests”, In: *3<sup>rd</sup> International Symposium on Cone Penetration Testing, CPT14*, Las Vegas, Nevada, 2014, pp. 47-73.
- [9] Schneider, J. A., Hotstream, J. N., Mayne, P. W., Randolph, M. F. “Comparing CPTU Q-F and  $Q-\Delta u_2/\sigma'_{v0}$  soil classification charts”, *Géotechnique Letters*, 2(4), pp. 209–215. <http://doi.org/10.1680/geolett.12.00044>
- [10] DIN 4094-1. „Baugrund, Felduntersuchungen, Teil1 1: Drucksondierungen“, Beuth, Berlin, 2002.
- [11] Kulhawy, F. H., Mayne, P. W. “Manual on estimating soil properties for foundation design”, Electric Power Research Institute, Palo Alto, California, Rep. EL-6800, 1990.
- [12] Benz, T. “Small-Strain Stiffness of Soils and its Numerical Consequences”, dissertation, Universität Stuttgart, 2007.
- [13] Schanz, T., Vermeer, P. A. „Angles of Friction and Dilatancy of Sand”, *Géotechnique*, 46(1), pp. 145-151.